Article

J. Mex. Chem. Soc. **2024**, *68*(3)
Regular Issue

ISSN-e 2594-0317

Experimental Studies to Optimize Process Parameters for the Removal of Cationic and Anionic Dyes by Natural Cypress Leaves

Oussama Larabi[1], Afaf Amara-Rekkab[1,2*], Mohamed Amine Didi[1], Amel Didi[1], Souad Feddane[1]

[1]Laboratory of Separation and Purification Technologies, Department of Chemistry — Faculty of Sciences, Box 119, University of Tlemcen — 13000, Algeria.
[2] Institute of Science and Technology, Department of Hydraulics, University center of Maghnia, Zouia maghnia street— 13000, Algeria.

***Corresponding author:** Afaf Amara-Rekkab, email: amarafaf@yahoo.fr; afaf.amara@cumaghnia.dz

Received March 30th, 2023; Accepted January 23rd, 2024.

DOI: http://dx.doi.org/10.29356/jmcs.v68i3.2037

Abstract. In this study, cypress leaves were used for the preparation of a biosorbent to remove brilliant green (BG) and black lanasyn (LB) from aqueous solutions. The influence of several experimental factors, such as time of contact, pH, initial concentration, ionic strength, temperature, stirring speed, and particle size, on the adsorption of these dyes was studied. Contact time s'effect has showed that balance was reached at 30 min with adsorption capacities 9.24 and 4.08 mg/g and elimination rates of 95.97 % and 34 % for BG and LB, respectively. Moreover, the study has shown that the adsorption of the two dyes can be described by pseudo-second-order kinetics. The adsorption isotherms demonstrated that the Freundlich model was satisfactory compared with the Langmuir model for describing the process of adsorption of the two dyes on the cypress. The results showed that the adsorption process is spontaneous, feasible, and endothermic for BG and non-spontaneous and exothermic for LB. Multi-docking reflecting the biosorption of brilliant green and Lanasyn black on the adsorbant surface is proposed. On the fundamental plane, the fractional orthogonal Taguchi plane L_{16} (4^5) was used to optimize the conditions for brilliant green adsorption on the cypress. In conclusion, the results showed that cypress leaves could be advantageously used as a low-cost biosorbent for the removal of brilliant green and lanasyn black in wastewater treatment.
Keywords: Brilliant green; lanasyn black; cypress leaves; adsorption; Taguchi method.

Resumen. En este estudio se usaron hojas de ciprés para preparar un biosorbente que remueve los colorantes verde brillante (BG) y lanasyn negro (LB) de soluciones acuosas. En la adsorción de estos colorantes se estudió la influencia de varios factores experimentales como tiempo de contacto, pH, concentración inicial, fuerza iónica, temperatura, velocidad de agitación y tamaño de partícula. El efecto del tiempo de contacto mostró que el balance se alcanzó a los 30 min con capacidades de adsorción de 9.24 y 4.08 mg/g y velocidades de eliminación de 95.97 % y 34 % para BG y LB, respectivamente. El estudio mostró que la adsorción de los dos colorantes se puede describir por una cinética de pseudo segundo orden. Para describir el proceso de adsorción de los dos colorantes en las hojas de ciprés, las isotermas de adsorción demostraron que el modelo de Freundlich es satisfactorio comparado con el modelo de Langmuir. Los resultados muestran que el proceso de adsorción es espontáneo, factible y endotérmico para BG, y no espontáneo y exotérmico para LB. Se propone un acoplamiento múltiple reflejando la biosorción del verde brillante y el lanasyn negro sobre la superficie del adsorbente. En el aspecto fundamental, la fracción ortogonal del plano de Taguchi L_{16} (4^5) se utilizó para optimizar las condiciones de adsorción del verde brillante en las hojas de ciprés. En conclusión, los resultados muestran que las hojas de ciprés pueden utilizarse como biosorbentes de bajo costo para la remoción de verde brillante y lanasyn negro en el tratamiento de aguas residuales.

J. Mex. Chem. Soc. **2024**, *68*(3)
Regular Issue

ISSN-e 2594-0317

Palabras clave: Verde brillante; lanasyn negro; hojas de ciprés; adsorción; método de Taguchi.

Introduction

The textile industry's need for various types of dyes used in clothing die and paper printing is a main source of water pollution [1]. Although dyes are present in only small amounts, they are highly detectable and thereby capable of causing various problems.

In addition, dyes are widely used in the textile, paper, plastic, and leather industries. Effluents discharged from these industries generally contain high concentrations of waste dyes. In addition, synthetic dyes can cause enormous environmental pollution, and pose a serious threat to human health [2-3]. For example, they cause severe headaches, profuse sweating, and other similar risks [4]. Therefore, the removal of dyes from wastewater is widely practiced in the industrial environment.

They are the first pollutants detected visually; however, because of their synthetic origin and mainly complex aromatic molecules, they are among the most difficult to remove. Most dyes are not directly or extremely toxic to living organisms [5]. For instance, brilliant green dye is an important dye in the paper printing and textile industries. Wood and silk materials, in particular, are dyed brilliant green. Its effluents are also generated by the rubber and plastic industries. This dye is hazardous in the case of skin contact, eye contact, and ingestion. It is toxic to the lungs by inhalation. Repeated or prolonged exposure to this substance may cause damage to the target organ. During its decomposition, it can generate carbon dioxide, sulfur oxides, and nitrogen oxides. Therefore, it is more important to remove the brilliant green dye from the aqueous solution [6].

Lanasyn black is an acidic metal complex azo dye. It is considered to be one of the most widely used and difficult to remove in wastewater [7].

Various physical, chemical, and biological techniques have been developed and tested to treat wastewater containing dyes, such as coagulation and agglomeration [8], biodegradation [9-10], membrane filtration [11-13], chemical oxidation [14], ozone treatment [15], ion exchange [16], electrochemical processes [17-20], and adsorption [21-23]. However, these processes are expensive and generate large quantities of sludge or derivatives.

Adsorption techniques are the cheapest methods to remove dyes, and they have become the analytical method of choice due to their high ability to purify contaminated water, high efficiency, and ease of use [24]. Biosorbents are the most commonly used materials because of their low cost. However, literature on the optimization of Brilliant green and Lanasyn black removal from aqueous solutions by the selected adsorbent using the Taguchi method design is not available.

Our work is based on the extraction of two dyes ("Brilliant green" cationic dye and "Black lanasyn" anionic dye) by a natural biosorbent, namely cypress leaves. The extraction technique used is liquid–solid extraction. Note that the adsorption of brilliant green and lanasyn black on different materials has been extensively investigated [25-34].

The analysis method used was UV-visible spectroscopy. The following parameters, stirring time, concentration effect, pH, ionic strength, salts (NaCl, Na_2SO_4, KBr, KNO_3), temperature, grain size, and stirring speed, were studied during this experiment to determine their influence on the extraction.

The effect of these experimental parameters on extraction was also studied by statistical treatment using the orthogonal array of $L_{16}(4^5)$ of Taguchi modeling.

Experimental

Preparation of the biosorbent

After collecting the cypress leaves from the tree, we washed them well with distilled water and left them to dry in the sun and then in an oven for 24 h at 60°C. After washing and drying, our biosorbent was ground and sieved as well as possible to a diameter of less than 0.2 mm, ready for use.

J. Mex. Chem. Soc. **2024**, *68*(3)
Regular Issue

ISSN-e 2594-0317

Dyes

Brilliant green (BG) and lanasyn black (LB) are used as dyes of analytical and practical grade, respectively. They were supplied to us by a textile factory (SOITEX) located in Tlemcen, Algeria. Their molecular structures are given in Scheme. 1.

(a) 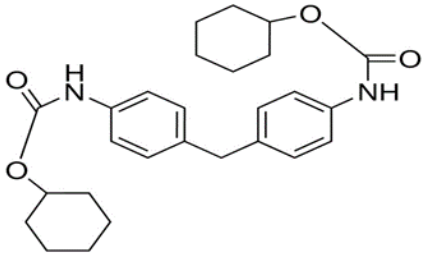

(b) 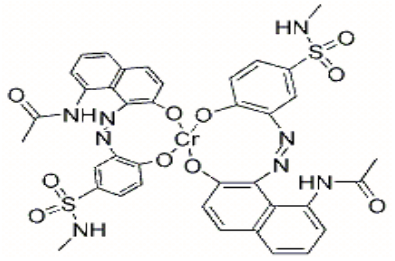

Scheme. 1. Chemical structure of BG **(a)** and LB **(b)**.

Preparation of the solutions

In a 1000 mL volumetric flask, 0.1 g of the brilliant green dye was added. 20 mL of distilled water was added to dissolve the dye, and the mixture was filled up to the mark. In another 500-mL volumetric flask, 0.05 g of black was introduced and adjusted to the gauge mark. For both dyes, solutions were prepared at different concentrations, namely 10, 15, 20, 25, 30, 35, 40, 45, 50 ppm by dilution.

Solutions of HNO_3 and NaOH were prepared by diluting HNO_3 (69 %) (AnalaR NORMAPUR) and dissolving appropriate amounts of NaOH (CARLA ERBA) in distilled water, respectively.

Previously calculated quantities of the salts NaCl (PROLABO), Na_2SO_4 (Sigma Aldrich), KNO_3 (Sigma Aldrich), and KBr (Sigma Aldrich) were dissolved in distilled water. The purity of all these compounds exceeds 99 %.

Equipment used

UV-visible spectrophotometer (Analytik Jena Specord 210 plus), pH meter (Adwa AD1030), centrifuge (Sigma 2-6), analytical balance (Pioneer TM), oven (Binder), mechanical stirrer with a speed controller (Haier), heating and stirring plate (Yellow Line), and sieve shaker (Orto Alresa) were used in our study.

Extraction procedure

The adsorption experiments were performed at different initial values of pH, temperature, and initial dye concentration. The tests were performed by shaking (at 250 rpm) 0.05 g of the cypress leaves in 10 mL of the synthetic solutions of the brilliant green and black dyes at concentrations varying from 10 to 50 ppm. The coloured solution was separated from the adsorbent by centrifugation at 4000 rpm for 10 min. The absorbance of the supernatant was measured using a UV/visible spectrometer at the wavelength that corresponds to the maximum absorbance of the BG (λ_{max} = 625 nm) and LB (λ_{max} = 575 nm). The residual dye concentration was determined using the calibration curve performed with a range of concentrations from 10 mg/L to 50 mg/L of BG and LB.

The adsorption capacity (Q) and adsorption yield of the dyes by the cypress leaves were calculated using Eq. (1) and (2):

$$Q\ (mg/g) = \frac{(C_0 - C) \times V}{m} \tag{1}$$

$$Biosorption\ yield\ (\%) = \frac{C_0 - C}{C_0} \times 100 \tag{2}$$

where C_0, C, V, and m are the initial concentration (ppm), equilibrium concentration (ppm), batch volume (L), and biosorbent mass, respectively.

J. Mex. Chem. Soc. **2024**, *68*(3)
Regular Issue

ISSN-e 2594-0317

Results and discussion

Determination of the point of zero charge pH_{pzc}

50 mL of NaCl (0.1 M) is put in a series of polypropylene bottles where the pH has been adjusted to precise values of 1–12 by the addition of 1 M NaOH or HCl. Then, 0.1 g of the adsorbent was added to each vial. The suspensions were kept under constant stirring at ambient temperature for 24 h to determine the final pH. The point of zero charge (pzc) corresponds to the intersection of the curve $\Delta pH = pH_f - pH_i$ as a function of pH_i with the abscissa axis.

Study of Adsorption

Effect of Agitation Time

Contact time is necessary to establish adsorption between the dye and the cypress biosorbent. This study was conducted to determine the fixed quantities of adsorbate dye from its first contact with the biosorbent until equilibrium is reached. For this, we followed the kinetics of adsorption of brilliant green and black lanasyn at initial concentrations of 20 and 50 ppm in contact with 0.1 g of cypress. The mixture was stirred at 25° C for varying durations ranging from 1 to 150 min. The yield curves of the adsorbed dyes as a function of time E (%)= f (Time) are presented in Figures 1 and 2.

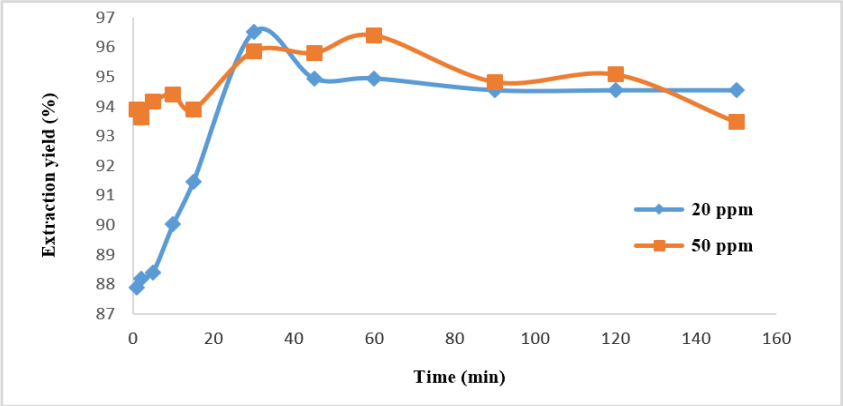

Fig. 1. Effect of time on BG extraction by cypress leaves, pH = 6.3, C_{BG1} = 20 ppm, C_{BG2} = 50 ppm, mass of biosorbent = 0.1g, $V_{solution}$ = 10 mL, and temperature = 18 °C.

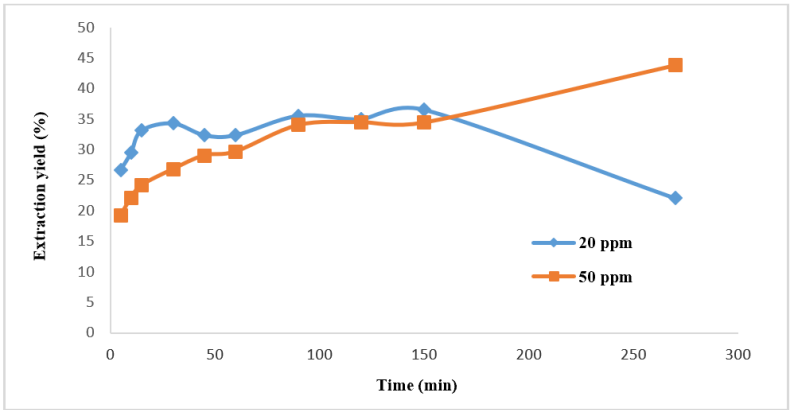

Fig. 2. Effect of time on LB extraction by cypress leaves, pH = 3.3, C_{LB1} = 20 ppm, C_{LB2} = 50 ppm, mass of biosorbent = 0.1 g, $V_{solution}$ = 10 mL, and temperature = 18 °C.

J. Mex. Chem. Soc. **2024**, *68*(3)
Regular Issue

ISSN-e 2594-0317

The study of the extraction yield as a function of the initial concentration, which is presented in Fig. 1, shows that the yield is better for the high concentration (50 ppm). It is observed that the increase in the initial concentration of BG causes a global increase in the adsorption of the dye. This is probably due to the saturation of cypress leaves active sites with the dye molecules, and consequently, the adsorption process decreased and finally reached equilibrium. The same observation was made in another research [24]. The opposite effect occurred in the case of LB adsorption, except for the high time of contact, Fig. 2.

Moreover, Fig. 1 shows that the adsorption is fast at the beginning of the process and becomes increasingly slow during the stirring time. The removal efficiency and adsorption capacity reached 95.97 % and 9.24 mg/g for a contact time of 30 min (equilibrium time), respectively.

From Fig. 2, we can note that the yield of the LB dye increases with stirring time, and the time required to reach equilibrium is 150 min with a removal efficiency of 34 % and an adsorption capacity q of 4.08 mg/g.

These contact times were fixed for the different dyes in the rest of the experiments. The high speed of adsorption in the first minutes of the reaction can be explained by the fact that at the start of adsorption, the number of active sites available on the surface of the absorbent is much greater than the sites remaining after some time. For high contact times, the molecules need time to diffuse inside the pores of the adsorbent. The remaining unabsorbed amount may be attributed to the saturation of the adsorbent surface [24].

Effect of pH

The initial pH of the coloured solutions is a crucial factor in controlling the adsorption process of cationic and anionic organic compounds. To evaluate the effect of the initial pH on the adsorption of the dyes studied, we chose coloured solutions at a concentration of 20 ppm with pH varying from 1 to 8. Acidification was achieved by the addition of a few drops of nitric acid HNO_3 1M. A solution of 1 M NaOH was used to make the medium basic.

Variations in the yield (%) of dye elimination as a function of the pH of the medium are presented in Fig. 3.

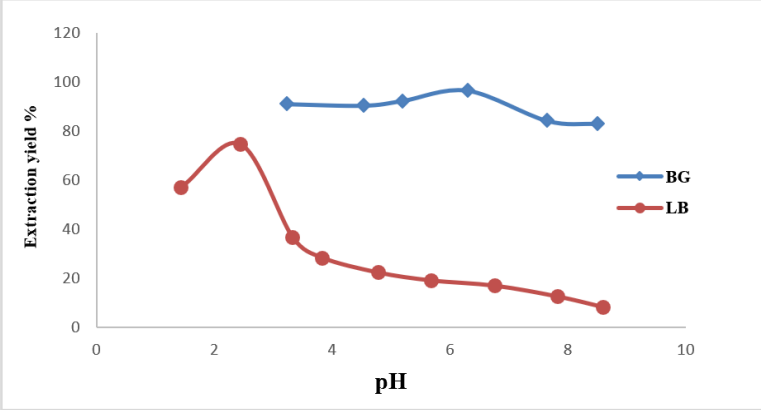

Fig. 3. Effect of pH on BG and LB extraction by cypress leaves, contact time: [30; 150 min], C_{BG} =C_{LB}=20 ppm, mass of biosorbent = 0.1g, $V_{solution}$ = 10 mL, and temperature = 18 °C.

The pH_{pzc} value of cypress leaves was 4.9. Consequently, at pH above the pH_{pzc} the adsorbent surface is negatively charged, favoring cation adsorption, anions adsorption is enhanced at pH below pH_{pzc}.

Fig. 3 highlights a slight increase in extraction yield when the pH is acidic. At pH 6, the BG adsorption yield reaches a maximum value of E equal to 96.52 %. We notice a strong decrease when the pH is strongly basic and higher than pH_{pzc} because of the repulsion between the negatively charged surface of the support and the molecules of the dye, which are also negatively charged. The biosorbent surface is slightly

J. Mex. Chem. Soc. **2024**, *68*(3)
Regular Issue

ISSN-e 2594-0317

acidic and positively charged when the pH of the solution is lower than pH_{pzc} and negatively charged when the pH of the solution is higher than pH_{pzc} [1]. In our case, pH_{pzc} is 4.9.

Concerning LB and from Fig. 3, we noticed that the extraction depends on the pH change of the aqueous phase. The extraction yield increases from 39.45 % to 78.45 % when the initial pH increases in parallel from 1.44 to 2.44. We notice also that the adsorption rate greatly decreased when the initial pH of the solution increased from 2.44 to 3.33. From the curve represented in Fig. 3, we can state that the best dye removal efficiency 78.45 % is obtained at pH equal to 2.44.

Finally, we can conclude that the variation in pH values reflects the effect of the chemical structure of the acid dye moieties on the adsorption process and their affinity for adsorption. The high affinity of the acid dye for the biosorbent is the result of ionic interactions between the anionic centers on the dye and the basic sites [35].

Effect of initial concentration

The effect of the initial concentration of the dye on the adsorption capacity of the different dyes on the "cypress" biosorbent was studied because of the significant influence of this parameter.

The concentration values vary between 10 and 100 ppm at a fixed room temperature for a contact time of 30 to 150 min. The results obtained from this study are shown in Fig. 4.

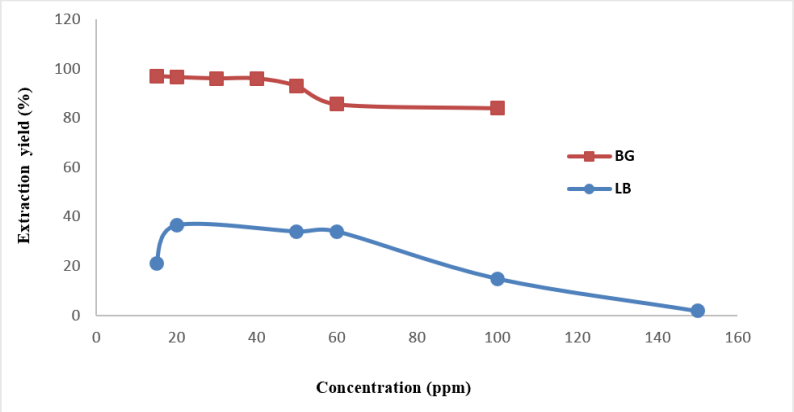

Fig. 4. Effect of initial concentration on BG and LB extraction by cypress leaves, contact time: [30; 150 min], pH= [6.3; 3.3], mass of biosorbent = 0.1 g, $V_{solution}$ = 10 mL, and temperature = 18 °C.

Fig. 4 shows that the LB adsorption capacity increases at low concentrations and reaches its maximum percentage at a concentration of 20 ppm, which corresponds to yields of 36.50 %, while the BG adsorption capacity decreases monotonously as the dye concentration increases. From these results, it can be concluded that the adsorption of dyes strongly depends on the initial concentration of the solution.

Effect of the ionic strength

The effect of ionic strength was studied using solutions of the following salts: NaCl, KNO_3, Na_2SO_4, and KBr at different concentrations. The results are shown in Figs. 5 and 6.

J. Mex. Chem. Soc. **2024**, *68*(3)
Regular Issue

ISSN-e 2594-0317

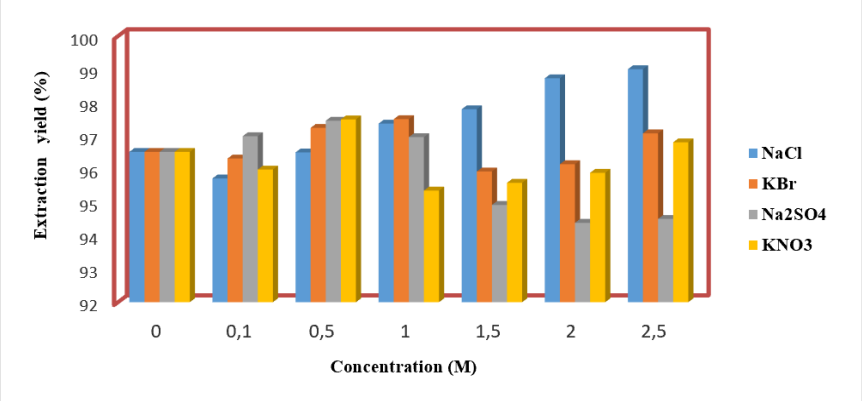

Fig. 5. Effect of ionic strength on BG extraction by cypress leaves, pH = 6.3, C_{BG} = 20 ppm, mass of biosorbent = 0.1g, $V_{solution}$ = 10 mL, and temperature = 18°C.

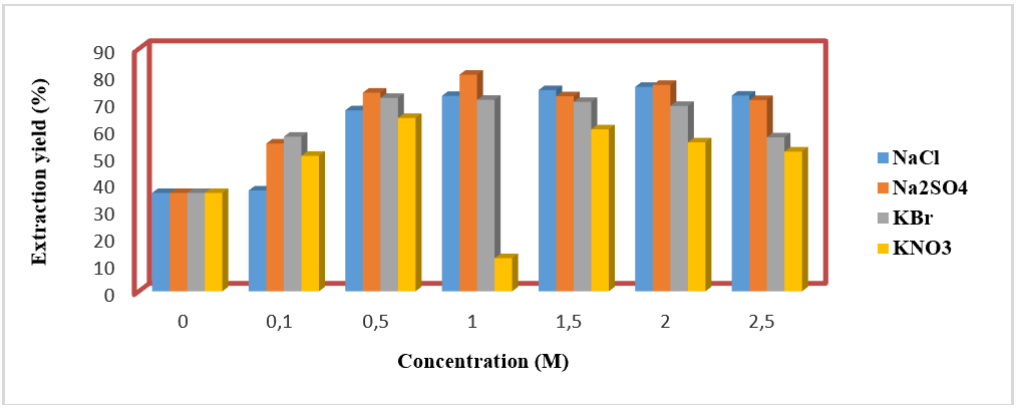

Fig. 6. Effect of ionic strength on LB extraction by cypress leaves, pH = 3.3, C_{LB} = 20 ppm, biosorbent mass = 0.1 g, $V_{solution}$ = 10 mL, and temperature = 18 °C.

As shown in Fig. 5, the addition of KBr and KNO_3 decreases the adsorbed amount of BG, whereas the presence of NaCl and Na_2SO_4 promotes its adsorption.

The increase in the adsorption of the dye on the biosorbents with the addition of NaCl and Na_2SO_4can then be attributed to the shielding of the repellent forces by the ionic force. This result is consistent with the literature that reports that when electrostatic forces are repulsive, an increase in ionic strength has a positive effect on adsorption [36]. We can also interpret these results using the Gouy Chapman theory on the double diffusion layer. This theory predicts that the thickness of this layer would be low with the ionic force, which facilitates the closeness of adsorbate molecules and particles. Furthermore, when NaCl is present in water, it dissolves easily. This results in a weakening of the bonds, so its hydrophobicity increases, which promotes dye adsorption [37].

Fig. 6 shows that the addition of the salts Na_2SO_4 and NaCl in the aqueous phase leads to an increase in the percentage of elimination of black lanasyn when the concentration in the aqueous phase of Na_2SO_4 and NaCl varies from 0 to 2.5 M, the extraction yield increases from 36.50 % to 80.39 % and from 36.50 % to 75.87 %, respectively. Therefore, the presence of Na^+ increases the extraction yield according to the Chatelier principle. Conversely, when adding KBr and KNO_3, there is a decrease in the rate of adsorption.

J. Mex. Chem. Soc. **2024**, *68*(3)
Regular Issue

ISSN-e 2594-0317

This result can be explained by an ionic competition between the cation K^+ and the anionic dye LB. This allows us to conclude that the salt that best promotes adsorption is indeed Na_2SO_4.

Temperature influence

To study the effect of temperature on the adsorption of BG and LB on the biosorbent, experiments were conducted at different temperatures from 20°C to 55°C. Fig. 9 represents the results obtained.

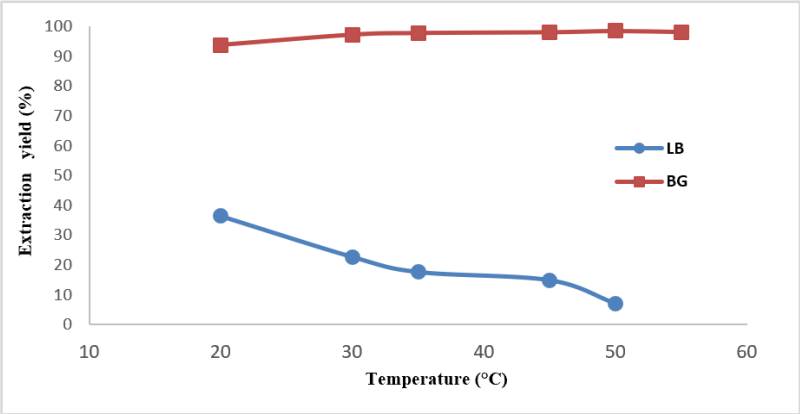

Fig. 7. Temperature effect on BG and LB extraction by cypress leaves, contact time: [30; 150 min], pH= [6.3; 3.3], C_{LB} = 20 ppm, C_{BG} = 20 ppm, mass of biosorbent = 0.1 g, $V_{solution}$ = 10 mL.

For the BG, it is noted from Fig. 7 that the increase in temperature causes an increase in the yield, i.e., the adsorption capacity. In this case, the phenomenon is endothermic ($\Delta H > 0$). The increase in adsorption with temperature is due to the increase in the solubility of the dye with the increase in temperature [37].
This figure also shows that an increase in the extraction temperature in the domain [20 °C – 50 °C] decreases the extraction yield of LB. This result can be attributed to the release of heat because $\Delta H < 0$ in this case.
To determine the different thermodynamic parameters (enthalpy: $\Delta H°$, entropy: $\Delta S°$ and free enthalpy: $\Delta G°$), we trace ln K_d as a function of 1/T:

$$\ln K_d = \frac{\Delta S°}{R} - \frac{\Delta H°}{RT} \quad (3)$$

This equation is drawn from the following equations:

$$\Delta G° = \Delta H° - T\Delta S° \quad (4)$$

$$\Delta G° = -RT \ln K_d \quad (5)$$

where R is the constant of perfect gases (R = 8.314 $J.mol^{-1}.K^{-1}$) and K_d is the distribution coefficient or partition coefficient of the two dyes BG and LB between the liquid and solid phases.
On the other hand, K_d is given by Eq. (6):

$$K_d = \frac{[C]}{[C]aq} \quad (6)$$

J. Mex. Chem. Soc. **2024**, *68*(3)
Regular Issue

ISSN-e 2594-0317

where [C] and $[C]_{aq}$ are the concentrations of the dyes BG and LB in both solid and the liquid phases at equilibrium, respectively.

The tracing of ln K_d as a function of 1/T allowed us to determine ΔH° and ΔS°.

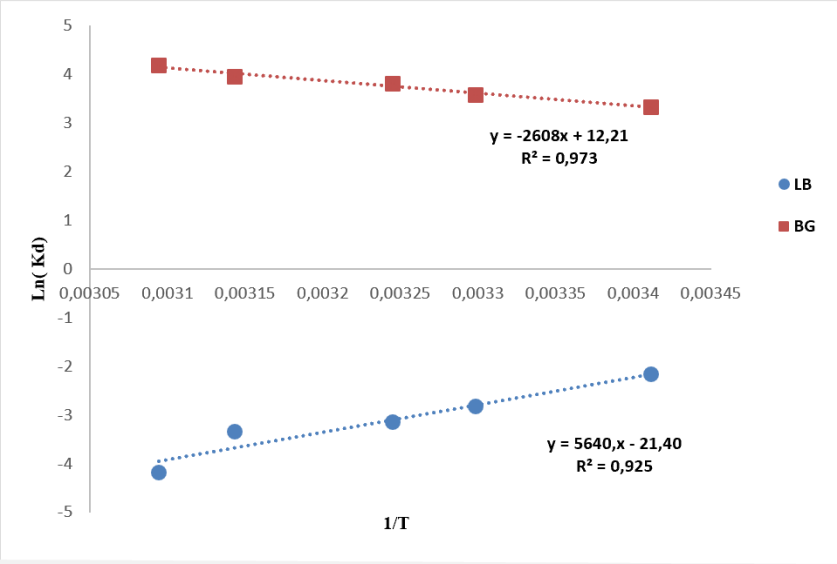

Fig. 8. Evolution of ln K_d as a function of 1/T for BG and LB, contact time: [30; 150 min], pH= [6.3; 3.3], C_{BG} = C_{LB} = 20 ppm, biosorbent mass = 0.1 g, $V_{Solution}$ = 10 mL, T= 18 °C.

The values of the enthalpie ΔH° and ΔS° were determined from the slopes and the ordinate at the origin of the obtained straight lines according to Eq. (3), respectively.

Table 1. Summarizes the calculated values of ΔH° and ΔS°, and ΔG° at different temperatures.

Dye	**ΔH° (kJ/mol)**	**ΔS° (J/mol.K)**	**ΔG° (kJ/mol)**				
			293.15 K	303.15 K	308.15 K	318.15 K	323.15 K
Brillant green	21.68	999.45	-8.096	-9.010	-9.763	-10.432	-11.242
Lanasyn black	-46.89	- 177.94	1.349	3.083	3.945	4.607	6.907

The values of ΔH°, ΔS°, ΔG° allow us to perform a thermodynamic analysis.

Indeed, the inspection of table 1 enabled us to notice the following:

- For BG, the positive sign of the enthalpy of extraction reflects the endothermic nature of BG extraction. Moreover, the positive value of ΔS° indicates that the molecular disorder has increased, and the negative value of ΔG° indicates that the extraction is a spontaneous process.
- For LB, the negative sign of the enthalpy of extraction reflects the exothermic nature of LB extraction. Moreover, the negative value of ΔS° indicates an increase in order during adsorption. Randomness decreases at the solid-solution interface during this binding process. This can be explained by the redistribution of energy between the adsorbent and the adsorbate.

J. Mex. Chem. Soc. **2024**, *68*(3)
Regular Issue

ISSN-e 2594-0317

Influence of stirring speed

To check the material transfer rate on the surface of the biosorbent, we tested different stirring rates, i.e., w = 0, 100, 150, 200, 250, and 300 rpm.

In adsorption processes, the stirring rate plays a crucial role in ensuring a good distribution of the adsorbent in the total volume of the adsorbate [36]. The results obtained are shown in Fig. 9.

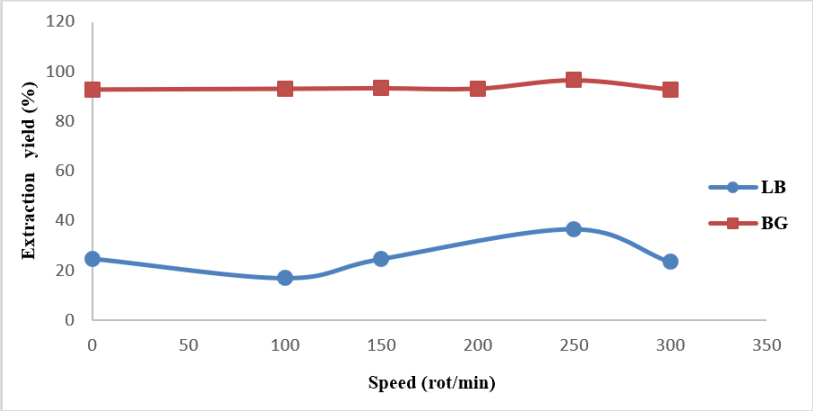

Fig. 9. Effect of stirring rate on BG and LB extraction by cypress leaves, contact time: [30; 150 min], pH= [6.3; 3.3], $C_{BG} = C_{LB}$=20 ppm, mass of biosorbent = 0.1 g, $V_{solution}$ = 10 mL. T=18 °C.

The results obtained from the study of the effect of the stirring rate on the adsorption of the two dyes on the cypress show that the maximum retention capacity is at a stirring speed of 250 rpm. Indeed, an average stirring speed of 250 rpm ensures good diffusion of the different dyes to the biosorbent used.

We can note that the homogenization of the mixture and a very high stirring rate reduce the contact between the dye and the support.

Effect of particle size

This effect has a significant impact on the adsorption capacity. In our study, five types of cypress particle sizes were used to study their effects on the adsorption of different dyes. Figures. 10 and 11 show the results obtained.

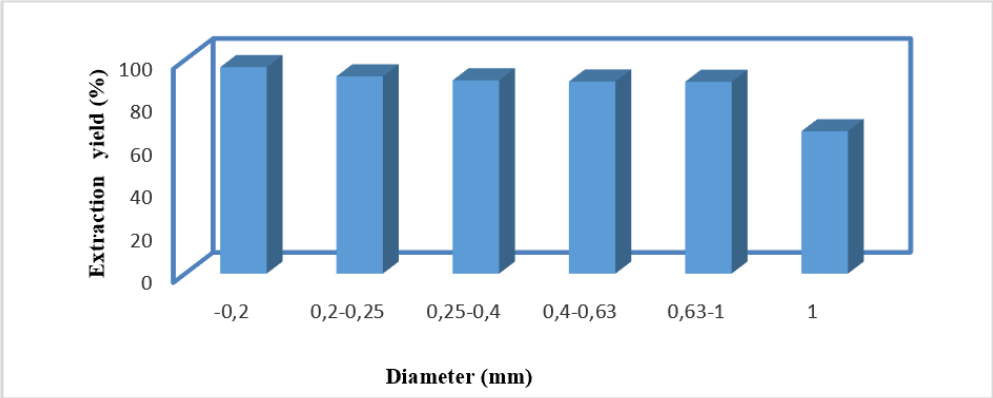

Fig. 10. Particle size effect on BG extraction of by cypress leaves, contact time = 30 min, pH = 6.3, C_{BG} = 20 ppm, biosorbent mass = 0.1 g, $V_{solution}$ = 10 mL, and temperature = 18 °C.

J. Mex. Chem. Soc. **2024**, *68*(3)
Regular Issue

ISSN-e 2594-0317

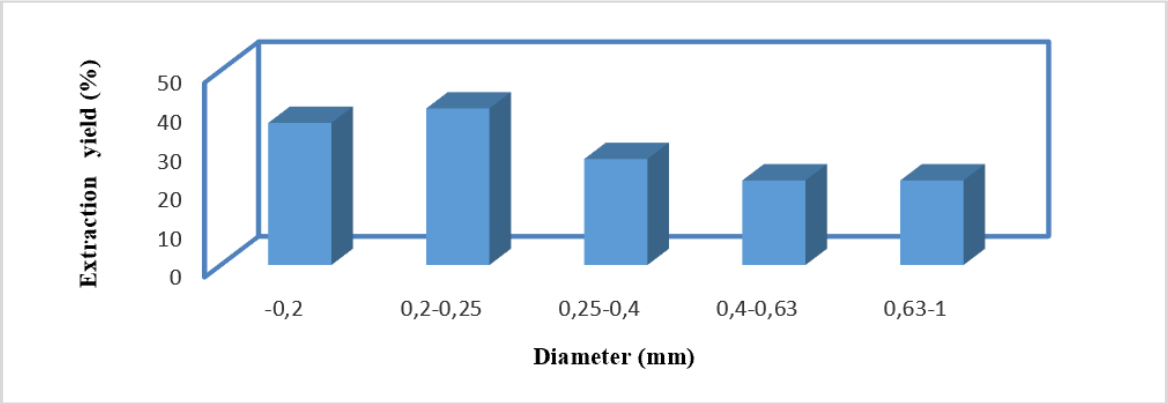

Fig. 11. Particle size effect on LB extraction by cypress leaves, contact time = 150 min, pH=3.3, C_{LB} = 20 ppm, biosorbent mass = 0.1g, $V_{solution}$ = 10 mL, and temperature = 18 °C.

These figures demonstrate that adsorption is significant and rapid for small samples, particularly in the case of BG. This could be explained by the fact that adsorption depends on the outer surface of the particles; the smaller the particle size, the larger the exchange surface, favoring a high rate of transfer from the dye to the adsorbent. In our work, the extraction yield was better for particle sizes of the order of 0.2 mm.

Models of kinetics

Several kinetic models were used to interpret the experimental data and provide essential information for the use of biosorbents in the adsorption domain. The most often used are pseudo-first-order and pseudo-second-order models [38].

Pseudo-first-order model

The expression is given by Lagergren:

$$\log (q_e - q_t) = \log (q_e) - (k_1 t/2.303) \quad (7)$$

where k_1 is the first-order reaction rate constant of the adsorption of BG or LB in (min), q_e is the amount of BG or LB adsorbed at equilibrium in (mg/g), q_t is the amount of BG or LB adsorbed at time t in (mg/g), and t is the contact time in (min).

Pseudo-second-order model

The pseudo-second-order model is given by the following expression [38]:

$$\frac{t}{q_t} = \frac{1}{k_2} * \frac{1}{q_e^2} + \frac{1}{q_e} * t \quad (8)$$

The results obtained for dye concentrations of 20 and 50 ppm are shown in Figs. 14 and 15:

J. Mex. Chem. Soc. **2024**, *68*(3)
Regular Issue

ISSN-e 2594-0317

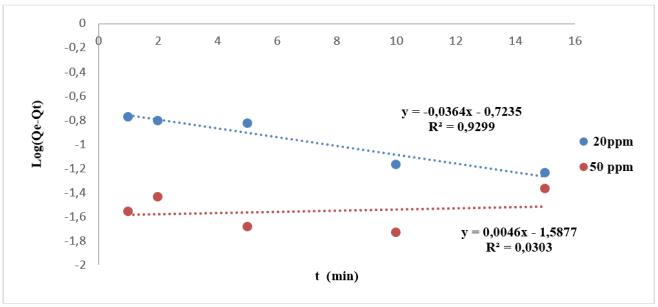

(a)

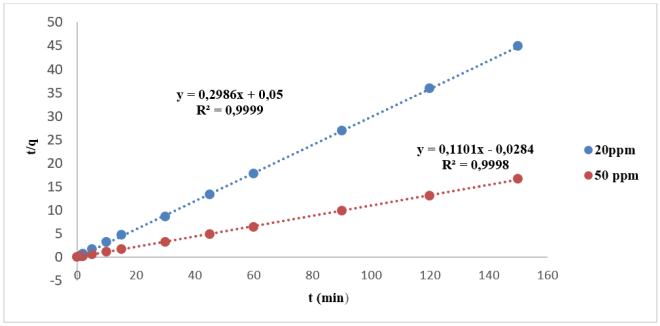

(b)

Fig. 12. (a) Pseudo-first-order, **(b)** pseudo-second-order kinetic modeling of BG adsorption on cypress leaves.

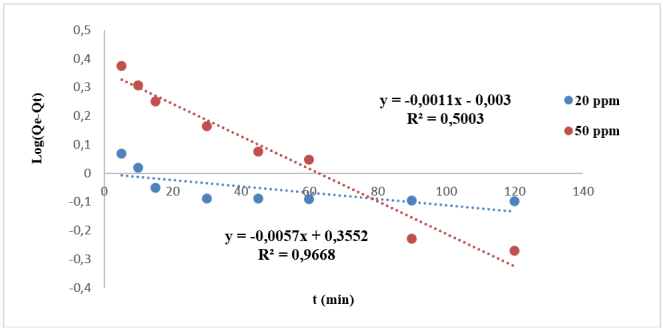

(a)

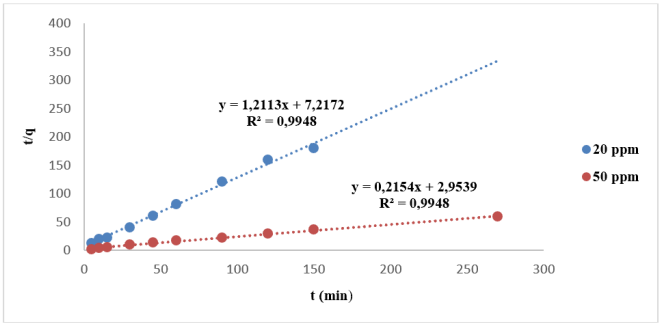

(b)

Fig. 13. (a) Pseudo-first-order, (b) pseudo-second-order kinetic modeling of LB adsorption on cypress leaves.

J. Mex. Chem. Soc. **2024**, *68*(3)
Regular Issue

ISSN-e 2594-0317

All parameters deducted from these figures and from the equation listed above are summarized in Table 2.

Table 2. Result of adsorption kinetics modeling for the two dyes.

	Brilliant green						**Lanasyn black**					
	First order			**Second order**			**First order**			**Second order**		
	q_e	k_1	R^2	q_e	k_2	R^2	q_e	k_1	R^2	q_e	k_2	R^2
20 ppm	0.485	0.0364	0.9299	3.3489	1.7833	0.9999	0.9931	0.0025	0.5003	0.8255	0.2033	0.9948
50 ppm	0.2043	-0.004	0.0303	9.0744	-0.362	0.9998	2.2656	0.0131	0.9668	4.6425	0.0157	0.9948

The results of the adsorption kinetics modeling for the dye BG mentioned in Table 2 show that the kinetic adsorption for the dye BG is of order 2, and that the adsorbed amount of the dye is better at a low concentration of 20 ppm. We also observe in Fig. 14 that for 20 ppm, the first and second orders are parallel to each other and stable over time, whereas for 50 ppm, the first and second orders differ slightly. Moreover, we note that the values of K decrease with increasing concentration.

Concerning LB, and according to the correlation values mentioned in Table 2 and Fig. 15, we can conclude that the 2nd order model is the most reliable and best for the concentration of 20 ppm. It is also observed that the value of K decreases with increasing concentration.

Isotherms of adsorption

Adsorption isotherms are an important aspect of assessing the adsorption capacity of a biosorbent and demonstrating its efficacy [39].

Several adsorption isotherms have been proposed in the literature to express the equilibria of a solute on the surface of a solid. Among these models, the Freundlich and Langmuir models were chosen.

Equilibrium (C_e) concentrations of BG and LB were quantified their adsorption mechanisms were elucidated using established nonlinear adsorption isotherms.

Langmuir Model

Langmuir's linear equation is:

$$\frac{c_e}{q_e} = \frac{1}{q_{max} * k_l} + \frac{c_e}{q_{max}} \tag{9}$$

where C_e is the residual concentration of the solute in the equilibrium solution (mg/L). q_e is the equilibrium adsorption capacity (mg/g), q_{max} is the maximum adsorption capacity (mg/g), and k_L is the Langmuir adsorption coefficient (L/mg) [40].

Freundlich model

The linear form of the equation is:

$$ln\ q_e = ln\, k_f + \frac{1}{n} ln\, c_e \tag{10}$$

where q_e is the equilibrium adsorption capacity (mg/g) .k_f is the Freundlich adsorption coefficient (L/mg), and Ce is the residual concentration of the solute in the equilibrium (mg/L) [41].

J. Mex. Chem. Soc. **2024**, *68*(3)
Regular Issue

ISSN-e 2594-0317

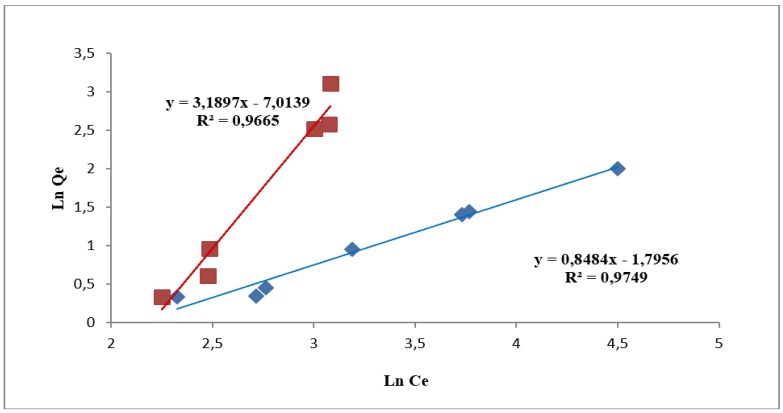

Fig. 14. Langmuir isotherm for the adsorption of BG and LB on cypress leaves.

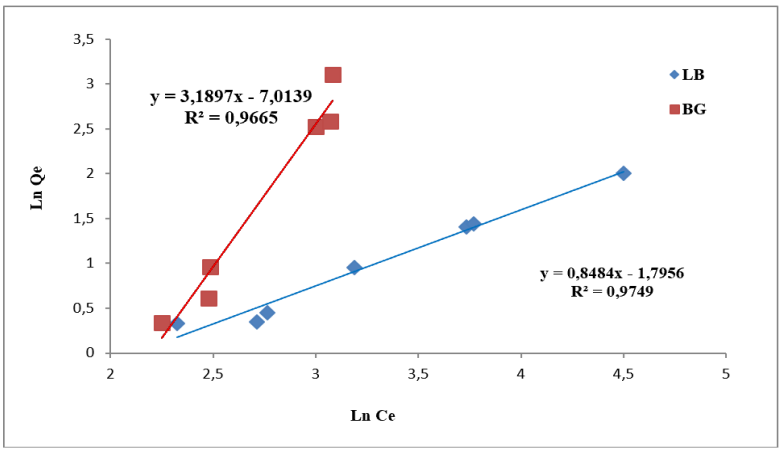

Fig. 15. Freundlich isotherm for the adsorption of BG and LB on cypress leaves.

The corresponding parameters are grouped in Table 3.

Table 3. Parameters of the Langmuir and Freundlich models for adsorption isotherm modeling of the two dyes on the biosorbent.

Langmuir						**Freundlich**					
Brilliant green			**Lanasyn black**			**Brilliant green**			**Lanasyn black**		
Q_m	**k_L**	**R_L^2**	**Q_m**	**k_L**	**R_L^2**	**1/n**	**R^2**	**k_f**	**1/n**	**R^2**	**K_f**
2.38	0.039	0.9387	37.593	$2.82*10^{-3}$	0.6412	3.1897	0.9665	$8.99.10^{-4}$	0.8484	0.9749	0.166

The results mentioned in Table 3 show that the modeling of adsorption isotherms at different concentrations of BG corroborates that the Freundlich model describes the experimental data of adsorption well.

J. Mex. Chem. Soc. **2024**, *68*(3)
Regular Issue

ISSN-e 2594-0317

For LB, the experimental values were adjusted for different isotherms such as Langmuir and Freundlich and are shown in Figs. 14 and 15. The different isotherm constants were evaluated, and the values of R^2 were close to 1.0. In the case of the Freundlich model, the best fit of the experimental data is given by the Freundlich isotherm. The n-value of the Freundlich isotherm was found to be greater than unity (n = 1.17). LB confirms the heterogeneity and greater affinity of LB toward the dye [42].

Characterization of the biosorbent

XRD characterization

For the cypress leaves, an intense diffraction peak was observed at 2θ = 15.51º and the other peaks were observed at 2θ = 21.93 and 24.94° (Fig. 16 **(a)**). Diffraction peaks for BG were observed at 2θ=15.45° and 24.91°. For the LB, they were observed at 2θ = 15.50º, 24.00º, 32.453º, 31º and 34.50º as shown in Figs. 16 **(b)** and 16 **(c)**. In comparing the latter with that of the cypress leaves composite, the peaks of cypress leaves-BG and cypress leaves-LB are moved toward the lower angles with the disappearance of the peak 2θ = 21.94 for BG and the appearance of two new peaks for LB at 2θ = 32.453 and 34.50. This confirms that the adsorption of the dyes is successful.

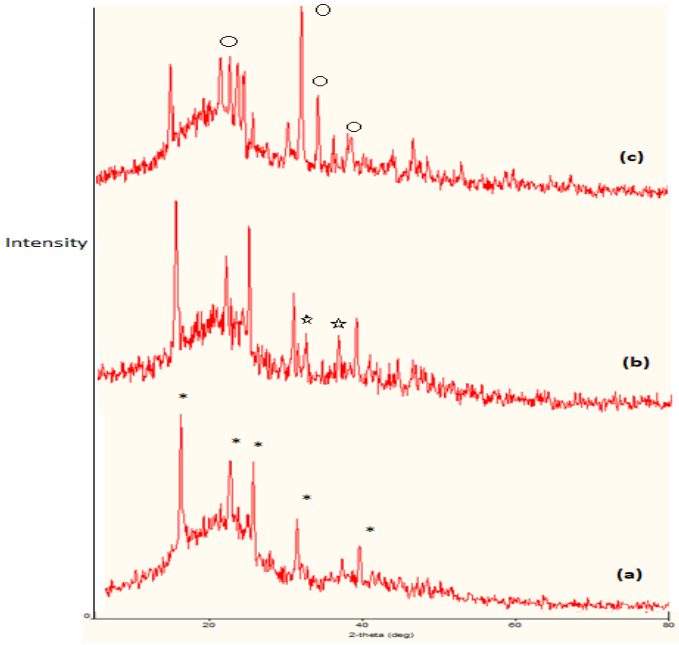

Fig. 16. XRD of cypress leaves **(a)** before, **(b)** after brilliant green adsorption, and **(c)** after lanasyn black adsorption.

Fourier transform infrared spectroscopy

As can be observed in Fig. 17 **(a)**, the strong and wide band with a maximum at 3400 cm^{-1} can be assigned to the vibrations of the –OH group linked in cellulose and lignin molecules or by adsorbed water [43]. Stretching vibrations of C-H and C-O bonds were attributed to the bands at 2922 cm^{-1} and 1618 cm^{-1}, respectively. The band around 1316 $cm^{-1}$was assigned to C-O stretching. The band at 1035 $cm^{-1}$was assigned to C-O stretching of cellulose present in cypress leaves. The band around 780 $cm^{-1}$was assigned to C-H bending. Furthermore, Fig.17 **(b)** and **(c)** show the spectra of BG-loaded and LB-loaded cypress leaves. A change is observed in the signal intensity of some bands and the displacement or appearance of other bands. These differences could be related to the possible involvement of specific functional groups on the cypress leaves surface during the adsorption process.

J. Mex. Chem. Soc. **2024**, *68*(3)
Regular Issue

ISSN-e 2594-0317

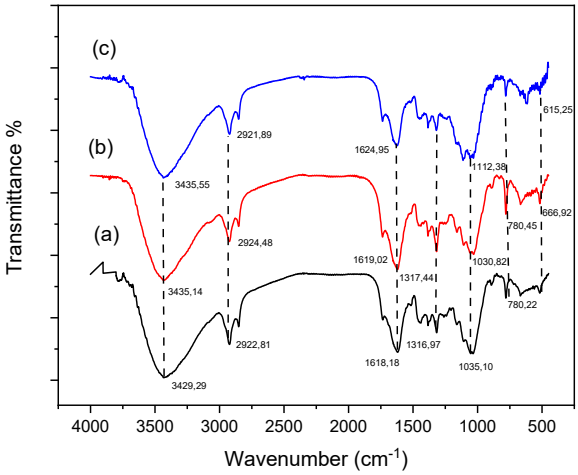

Fig. 17. FTIR spectra of cypress leaves **(a)** before, **(b)** after brilliant green adsorption, and **(c)** after lanasyn black adsorption.

Docking analysis of brilliant green and lanasyn black

Molecular docking studies were carried out to validate the experimental findings and locate the credible binding interfaces of ligands with the active sites of the enzymes of our biosorbent cypress leaves. Lectins were synthesized in our biosorbent previously [44]. Docking studies were performed using the AUTODOCK 4.2 program [45-47]. The structure of lectins was retrieved from the Protein Data Bank (PDB: 5Y42): https://www.rcsb.org/structure/5Y42 (Protein Plant). The 3D structures in PDB format of dyes were designed by Chemdraw data base and converted to PDB format using AutoDock Tools where the water molecules were removed, the polar hydrogen atoms were added to the amino acid residues. Then the protein in PDBQT format was used as an input for the AUTOGRID program. Rigid ligand docking was performed with using a blind docking. The results were shown using Discovery Studio Visualizer [46-48].

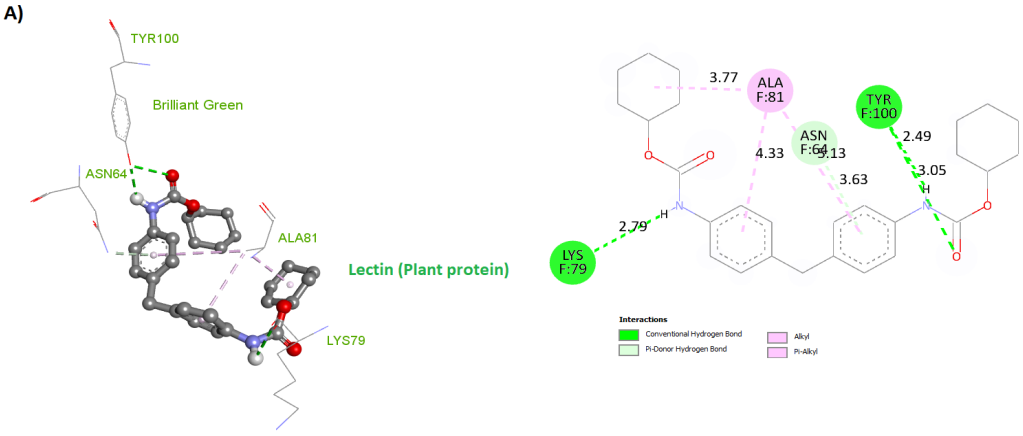

J. Mex. Chem. Soc. **2024**, *68*(3)
Regular Issue

ISSN-e 2594-0317

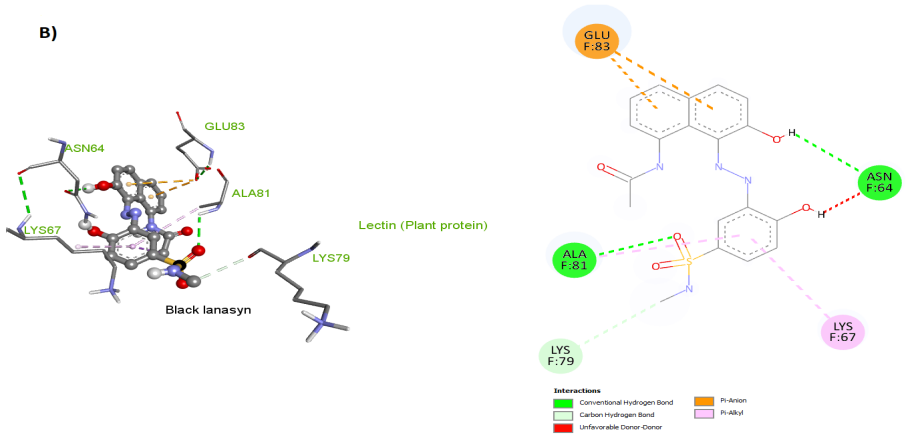

Fig. 18. 3D images of lectins of cypress leaves with (A) Brilliant green and (B) Lanasyn black.

Molecular docking allowed us to identify the different active sites of our biosorbent. Brilliant green complexed inside the active sites of lectins of cypress leaves, showing many important interactions, as presented in Fig. 18. It formed conventional hydrogen bonds with TRY 100 (2.49 and 3.05˚A) and LYS 79 (2.79˚A) amino acid residues of lectins. ASN 64 (3.63, 3.77 and 4.33°A) developed alkyl and pi-alkyl interactions with brilliant green. The ASN 64 residue stabilized the ligand by forming pi-doner hydrogen bond (3.13 ˚A) interactions.

Lanasyn black developed two converted hydrogen bonds: ASN 64 (4.59 ˚A), ALA 81 (3.74 ˚A), amino acid residues of the biosorbent. GLU 83 developed two π–anion (3.57 and 4.37˚A) interaction with the lanasyn black. Pi-alkyl interaction was developed (LYS 67: 4.86 ˚A) and carbon hydrogen bond interaction (LYS 79: 5.71 ˚A) with our biosorbent. The least binding energies between lectins and brilliant green and lanasyn black were -5.3 and - 5.6 Kcal/mol, respectively.

Application of the Taguchi methodology

The adsorption process can be influenced by several variables, such as the initial pH of the solution, adsorbent dose, adsorbate concentration, contact time, temperature, stirring speed, and parameters related to the state of the adsorbate and the adsorbent. Therefore, to achieve maximum contaminant removal, it is important to adopt an experimental design and optimize the process conditions. In this part, it is a question of applying the statistical approach of Taguchi to optimize the parameters of the process of adsorption of brilliant green by the leaves of cypress. In the Taguchi method,word optimization implies the determination of the best controllable factor levels. The best levels of controllable factors are those that maximize the signal-to-noise (S/N) ratios [43]. Given that our results showed that cypress leaves adsorb brilliant green better than lanasyn black, we preferred to apply the Taguchi methodology only for brilliant green.

The orthogonal table L_{16} (4^5) was chosen for the extraction of brilliant green by the cypress leaves. It is a matrix of experiments with 5 columns (5 factors at 4 levels each) and 16 rows, i.e., 16 experiments to be carried out.

Table 4. Parameters examined and their levels for the brilliant green dye.

Level	pH	[BG] (ppm)	NaCl (M)	Granulometry (mm)	Time (min)
1	3.3	20	0	< 0.02	1
2	4.8	40	0.5	0.25-0.4	15
3	6.3	60	1.5	0.4-0.63	30
4	7.8	80	2.5	1	60

J. Mex. Chem. Soc. **2024**, *68*(3)
Regular Issue

ISSN-e 2594-0317

Analysis of the results of the extraction of Brilliant green dye

In this study, we will follow the evolution of the extraction yields of the brilliant green dye by the biosorbent "cypress leaves." The latter requires sixteen (16) experiments.

The signal-to-noise ratio (S/N) is a performance indicator used by Taguchi. Determining the combination of the main effects that are important and evaluating their influence on responses (extraction yield). This ratio simultaneously takes into account the desired objective (the signal) and the dispersion of this value (noise). It is determined differently depending on the nature of the criterion studied.

In this study, we seek to maximize the signal/noise (S/N) ratio. This is calculated as follows:

$$\frac{S}{N} = -10\ log\left(\frac{1}{n}\sum_{i=1}^{n}\frac{1}{E_i^2}\right) \tag{11}$$

where n denotes the number of duplicates in each experiment (3 times) and E_i denotes the extraction yield in each experiment. We calculated the S/N ratio to identify the control and noise parameters.

Table 5. Experimental results for the adsorption of brilliant green by cypress leaves.

	pH	[BG] (ppm)	NaCl (M)	Granulometry (mm)	Time (min)	R_1 (%)	R_2 (%)	R_3 (%)	R_m (%)	S /N
1	1	1	1	1	1	79.92	84.25	80.00	81.39	38.21
2	1	2	2	2	2	61.00	75.41	71.73	69.38	36.82
3	1	3	3	3	3	76.30	69.42	72.60	72.78	37.23
4	1	4	4	4	4	32.06	36.20	34.13	34.13	30.66
5	2	1	2	3	4	38.01	42.14	42.15	40.77	32.21
6	2	2	1	4	3	86.48	90.06	87.68	88.08	38.90
7	2	3	4	1	2	86.63	85.71	75.74	82.70	38.35
8	2	4	3	2	1	94.20	92.02	92.73	93.00	39.36
9	3	1	3	4	2	71.00	67.92	68.00	69.00	36.77
10	3	2	4	3	1	40.09	44.50	39.98	42.84	32.64
11	3	3	1	2	4	66.00	67.74	67.02	66.91	36.51
12	3	4	2	1	3	95.90	98.33	93.78	96.00	39.65
13	4	1	4	2	3	92.51	89.21	92.71	91.50	39.23
14	4	2	3	1	4	90.00	89.90	93.76	91.05	39.19
15	4	3	2	4	1	62.64	62.68	64.66	63.33	36.04
16	4	4	1	3	2	56.00	48.71	54.87	53.11	34.50

We notice that the best interaction at experiment 12 was when pH was at level 3, concentration of BG at level 4, concentration of NaCl at level 2, particle size at level 1, and time at level 3.

J. Mex. Chem. Soc. **2024**, *68*(3)
Regular Issue

ISSN-e 2594-0317

Parameter effect calculations

The effect of a parameter is defined as the absolute value of the difference between the average of the ratios (S/N) of two levels i and j of the parameter. This translates mathematically into the following relationship:

$$\Delta(S/N)m = |[(S/N)m]j - [(S/N)m]i| \quad i<j \tag{12}$$

The parameter with the absolute value of the highest difference has the most significant effect on the response.

Table 6. Ratios (S/N) m and main effects of parameters for the adsorption of brilliant green on cypress leaves.

Level	pH	[Brilliant green](ppm)	[NaCl] (M)	Granulometry (mm)	Time (min)
1	35.72	36.60	37.02	38.86	36.54
2	37.22	36.90	36.2	38.00	36.60
3	36.40	37.02	38.15	34.16	38.76
4	37.25	36.03	35.22	35.60	34.65
Delta	1.51	1.00	2.5	4.71	4.12
Rank	4	5	3	1	2

The highest plots of each parameter were chosen, as shown in Fig. 19. The ratio was chosen because the larger the ratio, the better [40]. The same optimum conditions can be seen in Table 6 by the delta values. Therefore, particle size (mm) is the most influential parameter on the adsorption yield. The ranking of the parameters in descending order of their percentage contribution to the adsorption process is as follows: granulometry, time, concentration of NaCl, pH, and concentration of BG.

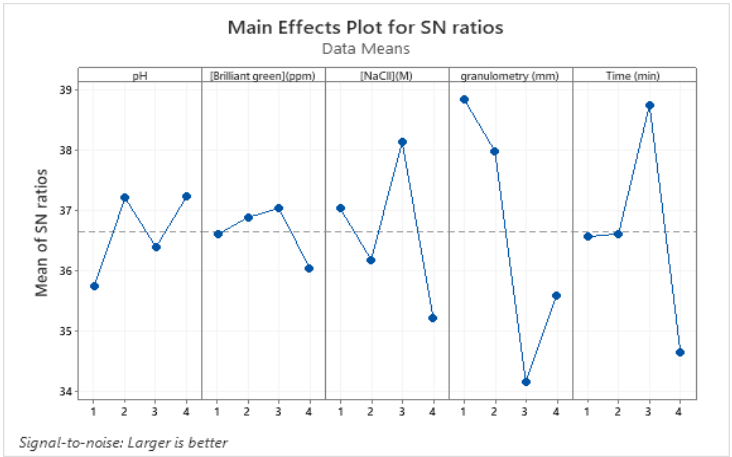

Fig. 19. Graphs of the main effects of signal/noise ratios for the adsorption of BG by cypress leaves.

The segments of the S/N ratios and the average extraction yields of the BG defined by the various factors studied present an aspect when moving from level 1 to level 4. Particle size and time are the most significant factors.

J. Mex. Chem. Soc. **2024**, *68*(3)
Regular Issue

ISSN-e 2594-0317

Analysis of variance (ANOVA)

Analysis of variance (ANOVA) is a statistical tool used to interpret the meaning and significance of experimental data and results.

The analysis of variance provides access to the optimal performance of the process parameters based on the determination of the significant differences between them. In the L_{16} Taguchi model, we used ANOVA to identify the main factors that could impact the adsorption of brilliant green. ANOVA can reveal the statistically significant change in process performance caused by a change in the level of a factor. The significant change was estimated by determining the F value (ratio of variance), and the contribution rate of each factor was calculated by the design parameters and error [48]. ANOVA was used to determine the sum of the squares of the factor (SS_F), the total sum of the squares (SS_T), the variance of error (VER), the mean of the MS squares, the associated F test of significance (5% of the risk), and the percentage of contribution of each factor (F). These quantities were calculated using equations 15 and 17 to 20. The results of the calculations are grouped in the table.

$$SS_F = \frac{mn}{L}\sum_{K=1}^{L}(\bar{E}_K^F - \bar{E}_T)^2 \tag{13}$$

E_T : is the cumulative average of extraction obtained by the L_{16} Taguchi design, given by Eq. (16).

$$\bar{E}_T = \sum_{j=1}^{m}\left(\sum_{i=1}^{n} E_i\right)_j /mn \tag{14}$$

where L is the number of levels of each factor and m is the experiment number carried from L_{16} Taguchi design.

$$SS_T = \sum_{j=1}^{m}\left(\sum_{i=1}^{n} {E_i}^2\right)_j - mn(\bar{E}_T)^2 \tag{15}$$

$$V_{Er} = SS_T - \sum_{F=A}^{D}\frac{SS_F}{m(n-1)} \tag{16}$$

$$MS = \frac{SS_F}{DF} \tag{17}$$

$$F - value = \frac{MS}{V_{Er}} \tag{18}$$

Table 7 shows that all parameters affect the color during the dyeing process. When the F-ratio is greater than the F-table, the hypothesis null is rejected and otherwise [49]. By comparing F-table F (0.05, 3, 3) = 9.28 to F ratios with the level of significance α = 5%. We found that all F- ratios above are greater than 9.28. Therefore, all factors affect the responses. Particle size has the biggest contribution to dye extraction, followed by factor time, NaCl concentration, and pH. Also, the main effect for the granulometry and the time of the extraction are statistically significant at the significance level of α = 0.05 (the p-value is less than the

J. Mex. Chem. Soc. **2024**, *68*(3)
Regular Issue

ISSN-e 2594-0317

significance level α). We can conclude that a change in these variables is associated with a change in the response variable.

Table 7. ANOVA Approach.

Source	DF	SS_F	MS	F-Value	P-Value	Contribution (%)
pH	3	356.56	118.85	11.97	0.036	6.01
[NaCl](M)	3	764.34	254.78	25.65	0.012	12.87
Granulometry (mm)	3	3070.28	1023.43	103.04	0.002	51.71
Time (min)	3	1716.29	572.10	57.60	0.004	28.91
Error	3	29.80	9.93	-	-	0.50
Total	15	5937.28	-	-	-	100.00

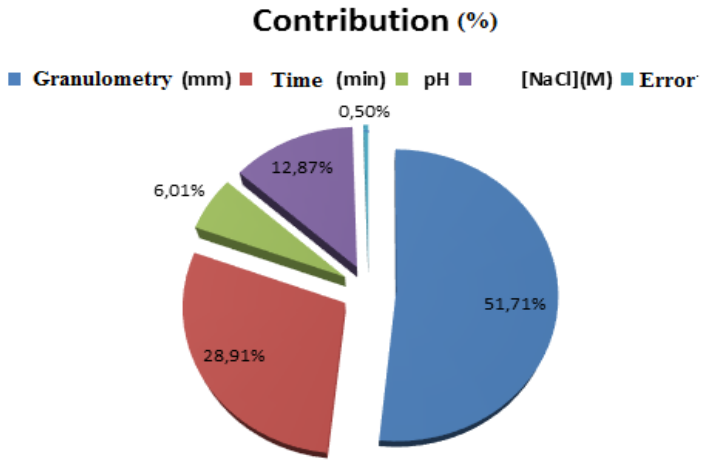

Fig. 20. Contribution of different parameters to the adsorption of brilliant Green on cypress leaves.

According to the results obtained, the particle size represent the largest contribution percentage. These results clearly indicate that the adsorption on the cypress leaves studied is considerably influenced by the particle size, contact time, ionic strength, and pH.

Contour plot of extraction yield

This contour plot shows the relationship between the variables for E_m (%) used for the extraction of BG from cypress leaves.

J. Mex. Chem. Soc. **2024**, *68*(3)
Regular Issue

ISSN-e 2594-0317

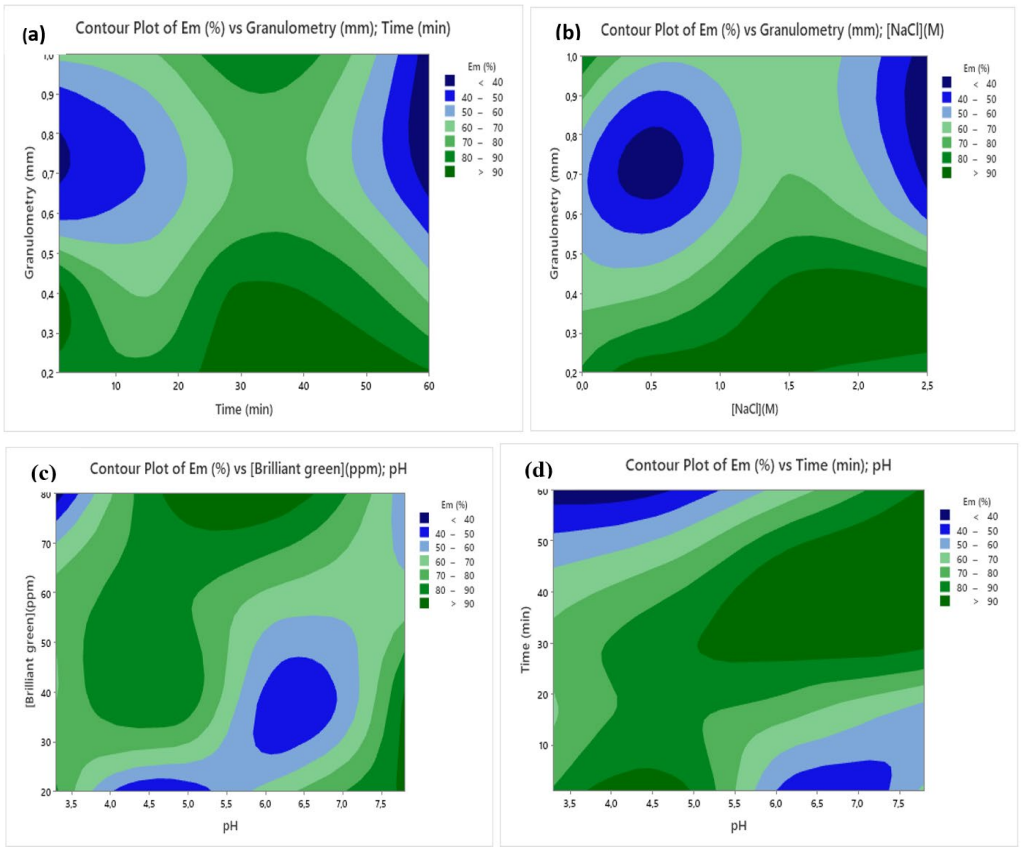

Fig. 21. Contour plots between variables for E_m (%). **(a)** Interactive effect of granulometry and time on Em (%). **(b)** Interactive effect of granulometry and NaCl concentration on E_m (%). **(c)** Interactive effect of pH and BG concentration on Em (%). **(d)** interactive effect of pH and time.

The contour plot lines signify the relationship and interaction effect of the two variables with varying E_m % on dye extraction. The third variable was appreciated at the middle level. These plots were created to learn about the changes in surface response. Plots are used to predict the extraction of the tested variables at different rates [50]. A contour plot indicates the type of interaction between the tested variables and the response.

Fig. 20 shows extraction up to 90 % in the broad pH range (5.2-8.0) with time (25–60 min), pH (4.7-6.5) with brilliant green concentration (73-80 ppm), NaCl concentration (0.25-2.5 M) with granulometry (0.2-0.45 mm), and time (23-50 min) with granulometry (0.2-0.4 mm).

Conclusions

The main conclusions drawn from these study areas follow:

- The pseudo-second order model is the most appropriate to describe the kinetics of the extraction of the brilliant green dye by the adsorbent cypress.
- An adequate model to describe the kinetics of lanasyn black extraction is the pseudo second order.
- As the dye concentration increases, the yield decreases.
- The extraction depends on the pH change of the aqueous phase.

J. Mex. Chem. Soc. **2024**, *68*(3)
Regular Issue

ISSN-e 2594-0317

- The salts that promote adsorption are NaCl for brilliant green and Na_2SO_4 for lanasyn black.
- The extraction yield increases with increasing temperature.
- The maximum retention rate was achieved at a stirring speed of 250 rpm.
- The increase in the particle size of the biosorbent decreases the yield.
- Brilliant green is more adsorbed in the range of concentration considered than lanasyn black.
- The application of adsorption isotherms shows that the adsorption of the two dyes follows the Freundlich model.
- The process is multi-docking, reflecting the biosorption of BG and LN on the cypress leaves, which were examined by determining the active sites of our biosorbent.
- The statistical study revealed that Taguchi's method with an L_{16} (4^5) orthogonal array design was successfully applied to the experimental optimization of brilliant green extraction.

Acknowledgements

This article is fondly and respectfully dedicated to Dear Professor Mohamed Amine DIDI, who has just left us on January 17, 2023. We will never forget you, Dear Professor.

References

1. Li, X.; Li, J.; Shi, W.; Bao, J.; Yang, X. *Mater*. **2020**, **13**, 332. DOI: https://doi/10.3390/ma13020332.
2. Aksu, Z.; Tezer, S. *Process. Bio. chem*. **2005**, **40**, 1347–1361. https://doi/10.1016/j.procbio.2004.06.007.
3. Forgacsa, E.; Cserhatia, T.; Oros, G. *Environ. Int*. **2004**, **30**, 953–971. DOI: https://doi/10.1016/j.envint.2004.02.001.
4. Bhattacharya, K. G.; Sharma, A. *Dyes. Pigm*. **2005**, **65**, 51–59. DOI: https://doi/10.1016/j.dyepig.2004.06.016.
5. Fernandez, M. E.; Nunell, G. V.; Bonelli, P.R.; Cukierman, A. L. *Bioresour. Technol*. **2010**, **101**, 9500–9507. DOI: https://doi/10.1016/j.biortech.2010.07.102.
6. Kismir, Y.; Aroguz, A. Z. *J. Chem. Eng*. **2011**, **172**, 199–206. DOI: https://doi/10.1016/j.cej.2011.05.090.
7. Belov, S.; Naumchik, G. *E3S. Web. Conf.* **2020**, **212**, 1-10. DOI: https://doi/10.1051/e3sconf/202021201001.
8. Papic, S.; Koprivanac, N.; Bozic, A. L. C. *Color. Technol.* **2000**, **116**, 352-358. DOI: https://doi/10.1111/j.1478-4408.2000.tb00013.
9. Adosinda, M.; Martins, M.; Nelson, L.; Silvestre, A. J. D.; Queiroz, M. J. *Chemosphere*. **2003**, **52**, 967–973. DOI: https://doi/10.1016/S0045-6535(03)00286-8.
10. López, C.; Valade, A. G.; Combourieu, B.; Mielgo, I.; Bouchon, B.; Lema, J. M. *Anal. Biochem.* **2004**, **335**, 135–149. DOI: https://doi/10.1016/j.ab.2004.08.037.
11. Calabro, V.; Pantano, G.; Kang, R.; Molinari, R.; Drioli, E. *Desalination*. **1990**,**78**, 257-277. DOI: https://doi/10.1016/0011-9164(90)80046-E.
12. Van Der Bruggen, B.; Lejon, L.; Vandecasteele, C. *Environ. Sci. Techn*. **2003**, **37**, 3733-3738. DOI: https://doi/10.1021/es0201754.
13. Anselme, C.; Jacobs, E. P. *Water treatment membrane processes, New York. McGraw Hill Mallevialle.* **1996**, 401-1087.
14. Andreozzi, R.; Caprio, V.; Insola, A.; Marotta, R. *Catal. Today*. **1999**, **53**, 51-59. DOI: https://doi/10.1016/S0920-5861(99)00102-9.
15. Koch, M.; Yediler, A.; Lienert, D.; Insel, G.; Kettrup, A. *Chemosphere*. **2002**, **46**, 109-113. DOI: https://doi/10.1016/S0045-6535(01)00102-3.

J. Mex. Chem. Soc. **2024**, *68*(3)
Regular Issue

ISSN-e 2594-0317

16. Leszczyěska, M.; Hubicki, Z. *Desalin. Water. Treat*. **2009**, **2**, 160–165. DOI: https://doi/10.5004/dwt.2009.254.
17. Brillas, E.; Mur, E.; Sauleda, R.; Sanchez, L.; Peral, J.; Domenech, X.; Casado, J. *Appl. Catal. B: Environ*. ***1998***, **16**, 31-42. DOI: https://doi/10.1016/S0926-3373(97)00059-3.
18. Oturan, M. A. *J Appl Electrochem*. **2000**, **30**, 477-478. DOI: https://doi/10.1023/A:1003994428571.
19. Boye, B.; Dieng, M. M.; Brillas, E. *Environ. Sci. Technol*. **2002**, **36**, 3030-3035. DOI: https://doi/10.1021/es0103391.
20. Bellakhal, N.; Dachraoui, M.; Oturan, N.; Oturan, M. A. *J. Soc. Chim. Tun*. **2006**, **8**, 223-228.
21. Lambert, S. D.; Graham, N. J. D.; Sollars, C. J.; Fowler, G. D. *Water. Sci. Technol*. **1997**, **36**, 173-180. DOI: https://doi/10.1016/S0273-1223(97)00385-5.
22. Lin, S. H. *J. Chem. Technol. Biotechnol*. **1993**, **57**, 387-391. DOI: https://doi/10.1002/jctb.280570415.
23. Ramakrishna, K. R.; Viraraghavan, T. *Water. Sci. Technol*. **1997**, **36**, 189-196. DOI: https://doi/10.1016/S0273-1223(97)00387-9.
24. Benamraoui, F. Master's thesis, Ferhat Abbas-Setif University, **2014**, Algeria.
25. Khalifah, A.; Hayfaa, A. M.; Amoako, J.; Laith, A. A.; Al Khaddar, R.; Mawada, A.; Al-Janabi, A.; Hashim, K. S. *Conf. Ser: Mater. Sci. Eng.* **2020**, **888**, 012036. DOI: https://doi/10.1088/1757-899X/888/1/012036.
26. Gul, S.; Azra, G.; Hajera, G.; Rozina, K.; Muhammad, I.; Khan, S.U.; Khan, M. S.; Aouissi, H. A.; Andrejs, Krauklis. *Mater*. **2023**, **2**, 1-15. DOI: https://doi.org/10.3390/ma16020521.
27. Baidya, K. S.; Upendra, K. S. *Afr. J. Chem. Eng*. **2021**, **35**, 33-43. DOI: https://doi.org/10.1016/j.sajce.2020.11.001.
28. Samiyammal, P.; Kokila, A.L.A.; Rajakrishnan, R.; Rengasamy, S.; Ragupathy, S.M. K.; Vasudeva, R.M.R. *Environ. Res.* **2022, 212**, 113497. DOI : https://doi.org/10.1016/j.envres.2022.113497.
29. Venkat, S.; Mane, P.V.; Vijay, B. *Desalination*. **2011**, **273**, 321-329. DOI: https://doi.org/10.1016/j.desal.2011.01.049.
30. Rehman, M. S.U.; Muhammad, M.; Muhammad, A.; Naim, R.; Muhammad, F.N.; Danish, M.; Han. *J. Chem. Eng*. **2013**, **228**, 54-62. DOI: https://doi.org/10.1016/j.cej.2013.04.094.
31. Nandi, B. K.; Amit, G.; Mihir, K, P. *J. Hazard. Mater*. **2009**, **161**, 387-395. DOI: https://doi.org/10.1016/j.jhazmat.2008.03.110.
32. Copaciu, F.; Virginia, C.; Mihaela, V.; Ocsana, O. *JPC-J. PLANAR. CHROMAT*. **2012**, **6**, 509-515. DOI: https://doi.org/10.1556/jpc.25.2012.6.4.
33. Amara-Rekkab, A. *Int. J. Health. Sci*. **2023,** **7**, 165–175. DOI: https://doi.org/10.53730/ijhs.v7n3.14657.
34. Belov, S.; Grigoriy, N. *E3S. Web. Conf*. **2020**, **212**, 01001. DOI: https://doi.org/10.1051/e3sconf/202021201001.
35. Samira, S.; DOMA, N. *H. Sci. Total. Environ*. **1989**, **79**, 71-279. DOI: https://doi/10.1016/0048-9697(89)90342-2.
36. Amara-Rekkab, A.; Didi, M.A. *Desalin. Water. Treat*. **2023**, **28**, 186–195. DOI: https://doi/10.5004/dwt.2023.29147.
37. Amara-Rekkab, A.; Didi, M.A. *J. Mater. Environ. Sci*. **2021**, **12**, 603-615.
38. Omri, A.; Benzima, M. *Desalin. Water. Treat*. **2012**, **51**, 2317- 2326. DOI: https://doi/10.1080/19443994.2012.734585.
39. Chandarana, H.; Ponnusamy, S. K.; Muthulingam, S.; Madhava, A. K. *Chemosphere*. **2021**, **285**, 131-480. DOI: https://doi/10.1016/j.chemosphere.2021.131480.
40. Langmuir, I. *J. Am. Che. Soc. J*. **1918**, **40**, 1361-1403. DOI: https://doi/10.1021/ja02242a004.
41. Freundlich, H. M. F. *Colloid and Capillary Chemistry*, *Methuen, London, UK*, **1926**.
42. Hossain, I.; Hossain, A.; Choudhury, I. A. *J. Text. Inst.* **2015**, **107**, 154-164. DOI: https://doi/10.1080/00405000.2015.1018669.
43. Savari, M.; Esfahani, S. H. Z.; Edalati, M.; Biria, D. *Protein. Expr. Purif*. **2015**, **114**, 128-135. DOI: https://doi/10.1016/j.pep.2015.06.006.
44. Necib, Y.; Bahi, A.; Merouane, F.; Bouadi, H.; Boulahrouf, K. *World. J. Pharm. Res*. **2015, 4**, 1720-1733.

J. Mex. Chem. Soc. **2024**, *68*(3)
Regular Issue

ISSN-e 2594-0317

45. Morris, G.; Huey, R.; Lindstrom, W.; Sanner, M.; Belew, R.; Goodsell, D.; Olson, A. *J. Comput. Chem*. **2009, 30**, 2785–2791. DOI: https://doi.org/10.1002/jcc.21256.
46. Kausar, N.; Murtaza, S.; Nadeem Arshad, M.; Munir, R.; Saleem, R. S. Z.; Rafique, H. T. *J. Mol. Struct.* 2021, 1244, 130983. DOI: https://doi.org/10 .1016/j.molstruc.2021.130983.
47. Bensegueni, R.; Guergouri, M.; Bensouici, C.; Bencharif, M. *J. Rep. Pharm. Sci*. 2019, 8, 195-203. DOI: https://doi.org/10.4103/jrptps.JRPTPS_46_18.
48. Asghar, A.; Abdul Raman, A. A.; Wan Daud, W. M. A. A. *Sci. World. J.* **2014**, 1-14. DOI: https://doi/10.1155/2014/869120.
49. Montgomery, D. C.; Runger, G. C. *Applied. Ed., John Wiley & Sons, Singapore*, **2014**.
50. Mohana, S.; Shrivastava, S.; Divecha, J.; Madamwar, D. *Bioresour. Technol*. **2008**, 99, 562–569. DOI: https://doi/10.1016/j.biortech.2006.12.033.